Acta Oceanol. Sin., 2023, Vol. 42, No. 1, P. 91–102
https://doi.org/10.1007/s13131-022-2098-x
http://www.aosocean.com
E-mail: ocean2@hyxb.org.cn

Sedimentary record of climate change in a high latitude fjord—Kongsfjord

Hang Wu[1], Binbin Deng[2], Jinlong Wang[1]*, Sheng Zeng[1], Juan Du[3], Peng Yu[4], Qianqian Bi[1], Jinzhou Du[1]

[1] State Key Laboratory of Estuarine and Coastal Research, East China Normal University, Shanghai 200241, China

[2] Monitoring Center of Aquatic Environment of Pearl River Basin, Guangzhou 510611, China

[3] Research Centre for Eco-Environmental Engineering, Dongguan University of Technology, Dongguan 523808, China

[4] Big Data Institute of Digital Natural Disaster Monitoring in Fujian, Xiamen University of Technology, Xiamen 361024, China

Received 26 May 2022; accepted 15 August 2022

Abstract

The sedimentary record of climate change in the Arctic region is useful for understanding global warming. Kongsfjord is located in the subpolar region of the Arctic and is a suitable site for studying climate change. Glacier retreat is occurring in this region due to climate change, leading to an increase in meltwater outflow with a high debris content. In August 2017, we collected a sediment Core Z3 from the central fjord near the Yellow River Station. Then, we used the widely used chronology method of ^{210}Pb, ^{137}Cs, and other parameters to reflect the climate change record in the sedimentary environment of Kongsfjord. The results showed that after the mid-late 1990s, the mass accumulation rate of this core increased from 0.10 g/(cm^2·a) to 0.34 g/(cm^2·a), while the flux of ^{210}Pb$_{ex}$ increased from 125 Bq/(m^2·a) to 316 Bq/(m^2·a). The higher sedimentary inventory of ^{210}Pb$_{ex}$ in Kongsfjord compared to global fallout might have been caused by sediment focusing, boundary scavenging, and riverine input. Similarities between the inventory of ^{137}Cs and global fallout indicated that terrestrial particulate matter was the main source of ^{137}Cs in fjord sediments. The sedimentation rate increased after 1997, possibly due to the increased influx of glacial meltwater containing debris. In addition, the ^{137}Cs activity, percentage of organic carbon (OC), and OC/total nitrogen concentration ratio showed increasing trends toward the top of the core since 1997, corresponding to a decrease in the mass balance of glaciers in the region. The results of δ^{13}C, δ^{15}N and OC/TN concentration ratio showed both terrestrial and marine sources contributed to the organic matter in Core Z3. The relative contribution of terrestrial organic matter which was calculated by a two-endmember model showed an increased trend since mid-1990s. All these data indicate that global climate change has a significant impact on Arctic glaciers.

Key words: Kongsfjord, radionuclide, organic carbon/total nitrogen (OC/TN) concentration ratio, δ^{13}C, δ^{15}N, sediment record, climate change

Citation: Wu Hang, Deng Binbin, Wang Jinlong, Zeng Sheng, Du Juan, Yu Peng, Bi Qianqian, Du Jinzhou. 2023. Sedimentary record of climate change in a high latitude fjord—Kongsfjord. Acta Oceanologica Sinica, 42(1): 91–102, doi: 10.1007/s13131-022-2098-x

1 Introduction

Global warming will result in the melting of glaciers, permafrost warming, sea-level rise, and seafloor methane release (Andreassen et al., 2017; Christiansen et al., 2010; Hodgkins et al., 2016). According to the forecast made by the Intergovernmental Panel on Climate Change (https://www.ipcc.ch/) in 2018, the global temperature will increase by 1.5℃ in 2052 relative to pre-industrial levels. The Arctic is highly sensitive to climate change; for instance, the air temperature in the Arctic increased by an average of 2.7℃ from 1971 to 2017 (Box et al., 2019). As a result of global warming, ice sheets and glaciers have retreated around Greenland since the 1990s (Mottram et al., 2019). Consequently, deltas in Greenland have advanced because of the increased mass loss from land-based ice (Bendixen et al., 2017). It has been reported that climatic variation exerts a stronger control on the spatiotemporal variability in the erosion rates of glaciers than ice dynamics (Koppes et al., 2015). It is important to investigate the sedimentary record with respect to climate change to understand the glacier-fed coastal environment (Boldt et al., 2013; Cowan et al., 2010). Due to global warming and glacial ablation, the sedimentation rate and concentrations of carbon, nitrogen, and heavy metals in the Arctic region are expected to vary over time.

Chronologies of ^{210}Pb and ^{137}Cs have been widely used in dating recent sediments. The ^{210}Pb method was first used by Goldberg (1963) and was then introduced into sediment research for lakes and bays (Koide et al., 1972; Krishnaswamy et al., 1971). The ^{210}Pb within sediment samples can be classified as "excess ^{210}Pb" (^{210}Pb$_{ex}$) and "supported ^{210}Pb". Both originate from the decay of ^{238}U in soil and rock. During the decay of ^{238}U, some gas products such as ^{222}Rn ($T_{1/2}$ = 3.8 d) escape to the atmosphere and produce ^{210}Pb, which then return to Earth's surface as ^{210}Pb$_{ex}$ via wet and dry deposition. The existence time and deposition rate of sediment can be measured using the exponential decay

Foundation item: The National Natural Science Foundation of China under contract Nos 42107251 and 41706089; the Natural Science Foundation of Fujian Province under contract No. 2020J05232.
*Corresponding author, E-mail: jlwang@sklec.ecnu.edu.cn

law of $^{210}Pb_{ex}$ (Sanchez-Cabeza and Ruiz-Fernández, 2012). As an artificial radionuclide, ^{137}Cs mainly originates from atmospheric nuclear tests, nuclear accidents (e.g., Chernobyl), nuclear reprocessing facilities, and nuclear power plants. The following two time marks can be used to date a specific sediment layer and calculate the average sedimentary rate: 1963, when ^{137}Cs of global fallout reached a maximum value; and 1952, when ^{137}Cs was first introduced into the environment.

Kongsfjord is located in the western part of Spitsbergen, Svalbard Archipelago, and is not completely covered by sea ice in winter (Wickström et al., 2020). The input of terrestrial material to Kongsfjord is mainly controlled by glaciers, and seawater becomes obviously stratified during the melting season (Walkusz et al., 2009). Previous studies have investigated the sedimentary rate in part of Kongsfjord (Aliani et al., 2004; Koziorowska et al., 2017; Kuliński et al., 2014; Mohan et al., 2018; Zaborska et al., 2006). Mohan et al. (2018) reported that the sedimentation rate had changed over the past two decades. However, the record of climate change in the sedimentary environment of Kongsfjord remains unclear. This study investigates the sedimentation rate variation during recent decades and attempts to reveal climate change using environmental parameters.

2 Materials and methods

2.1 *Study area*

Kongsfjord is a glacial fjord located in the European Arctic on the west Svalbard (74°–81°N, 10°–35°E). It is 20 km long and 4–10 km wide with several small islands (Svendsen et al., 2002). As a part of the Kongsfjord-Krossfjorden system, Kongsfjord is surrounded by the West Spitsbergen Current (WSC), Spitsbergen Trough Current (STC), and Spitsbergen Polar Current (SPC) (Nilsen et al., 2016). Atlantic water flows into Kongsfjord throughout the year, whereas there is less exchange between fjord water and open seawater during the winter (Berge et al., 2015; Husum et al., 2019). Kongsfjord, including Kongsvegen, Kongsbreen, and Kronebreen, is affected by valley glaciers and tide-related glaciers (Fig. 1). During the meltwater season, large volumes of meltwater and glacial debris are transported into the fjord system through subglacial discharge (Lydersen et al., 2014; Zajaczkowski, 2008), which subsequently rises (lighter density) to the surface at the glacier front, and become meltwater plumes, which contain suspended sediments. Rivers also contribute some meltwater and sediment to the fjord, for example, the Bayelva River in Ny-Ålesund, which is the largest river in the area.

2.2 *Sampling and analysis*

In August 2017, due to the limitation of the weight of core sampler and relative deep-water depth (117 m), we collected a short sediment core with a length of 9.5 cm (Core Z3, Fig. 1) from Kongsfjord (78°55′28.56″N, 12°08′30.54″E). It was then sliced at 0.5 cm intervals using a stainless-steel knife, and the obtained sediment samples were stored in resealable plastic bags at 4℃ awaiting laboratory analysis. The samples were subsequently freeze-dried. After freeze-drying, each sample was ground and homogenized before being sealed in a 10 mL plastic centrifuge tube for at least 21 d to establish a secular equilibrium between ^{226}Ra and daughter products of ^{222}Rn before measurement. The activities of $^{210}Pb_{ex}$ and ^{137}Cs in each sediment sample were measured using the methods described by Du et al. (2010) and an HPGe γ-ray spectrometer (GCW3522S, 35% relative counting efficiency and energy resolution of 1.8 keV at 1 332 keV). The activity of total ^{210}Pb (i.e., excess $^{210}Pb_{ex}$ and supported ^{210}Pb) was calculated from the area of 46.5 keV (4.25%) at the γ-spectrum. The supported ^{210}Pb activity was taken as the ^{226}Ra activity, which was determined from the gamma peaks of 351.9 keV (37.6%; ^{214}Pb) and 609.3 keV (46.1%; ^{214}Bi). Therefore, the $^{210}Pb_{ex}$ activity of each sediment sample was obtained by subtracting the ^{226}Ra activity from the total ^{210}Pb activity. The ^{137}Cs activity was detected at 661.6 keV (85.1%). All determined values were decay-corrected to the sampling date.

The percentage of organic carbon (OC) and total nitrogen (TN) in each dried sediment sample (ground and homogenised) was determined using a Vario EL III analyser. First, 5–10 mg of each sediment sample was added to a silver boat and mixed with 1 mol/L HCl until no gas was created to remove the inorganic carbon. Then, the sample was dried and packaged in a silver boat to detect the percentage of OC and $\delta^{13}C$. For the percentage of TN and $\delta^{15}N$ measurement, the dry sample (without acidification) was packaged into a tin boat and wait for measurement.

$\delta^{15}N$ and $\delta^{13}C$ values were determined using a Finnigan MAT 252 mass spectrometer connected to a Flash EA 1112 analyser.

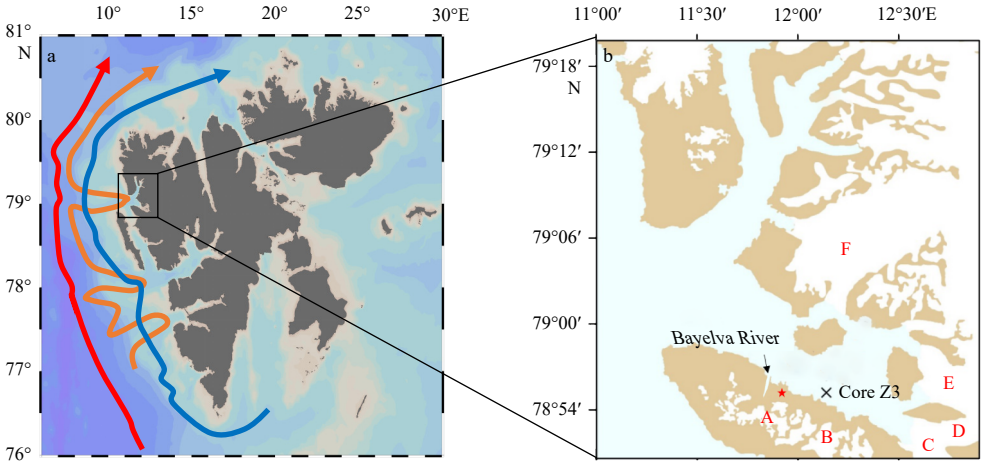

Fig. 1. Map of Kongsfjord showing the sampling station and major glaciers. The lines in a represent the ocean currents: West Spitsbergen Current (red line), Spitsbergen Trough Current (orange line), and Spitsbergen Polar Current (blue line). The black cross in b represents the station and the red English letters mean glaciers (A: Brøggerbreen; B: Lovénbreane; C: Kongsvegen; D: Kronebreen; E: Kongsbreen; F: Blomstrandbreen). The pentagram represents Ny-Ålesund.

$\delta^{13}C$ is given as the per mil deviation from the isotopic composition of the Vienna Pee Dee Belemnite standard. $\delta^{15}N$ is given as the per mil deviation from the N isotope composition of atmospheric N_2.

To measure the grain size of the sediment, 0.1–0.2 g of each dried sediment sample was first mixed with 5 mL of 10% H_2O_2 and 5 mL of 0.2 mol/L HCl to remove organic matter and metal oxide coatings. To completely disaggregate the sediments, 10 mL of 0.5 mol/L sodium hexametaphosphate solution was then added. After 24 h of reaction, the samples were placed in an ultrasound water bath for 10 min. The grain size of the sediment was subsequently detected using an MS-2000 laser particle analyser (Malvern Panalytical Company).

3 Results

3.1 *Grain size, C and N isotopes of sediment*

The basic parameters of all measurements were listed in Table 1. The overall distribution of Core Z3 was relatively uniform and its color was reddish brown. The main components of Core Z3 were clay and silt, which accounted for more than 85% (Fig. 2a). In Core Z3, the sand content and mean grain size first decreased and then increased with increasing depth from the top to the bottom of the core (Figs 2b, c). The highest mean grain size was observed in the last section, similar to the sand content. The $\delta^{13}C$ values showed a sub-maximum in the surface part of the core and ranged from –20.58‰ to –23.65‰, while $\delta^{15}N$ ranged from 4.39‰ to 5.55‰ (Figs 2e, f). The OC concentration ranged from 0.28% to 0.83%, with the maximum at the top of the core. The OC/TN concentration ratio ranged from 4.89 to 11.65, with the maximum was also observed at the top of the core (Fig. 2d)

3.2 *Radionuclides ^{210}Pb and ^{137}Cs*

The total ^{210}Pb activity ranged from 132 Bq/kg to 64 Bq/kg, with the maximum value observed in the top layer. A decreasing trend was observed from the surface to the bottom, and the minimum total ^{210}Pb activity occurred in the bottom layer. The $^{210}Pb_{ex}$ activity ranged from 94 Bq/kg to 33 Bq/kg and followed the same trend as the total ^{210}Pb activity. The ^{226}Ra activity did not fluctuate significantly and ranged from 30 Bq/kg to 41 Bq/kg. The ^{137}Cs activity ranged from 2.7 Bq/kg to 1.5 Bq/kg, with the maximum and minimum values observed in the 4.0–5.0 cm layer and 7.5–8.0 cm layer, respectively.

4 Discussion

4.1 *Sediment fluxes*

Atmospheric ^{210}Pb returns to Earth's surface via wet and dry deposition, providing a crucial source of ^{210}Pb to the global surface environment. With the melting of glaciers, debris and absorbed $^{210}Pb_{ex}$ are transported to Kongsfjord by meltwater. Among the sediment components, fine fraction (silt and clay) dominates the fjord system (>80%) (Choudhary et al., 2020). The sediment in inner part of Kongsfjord was mainly transported by two ways: ice-water rivers and broken-icebergs. The former deposited coarse debris and transported the fine particles to the fjord. The latter quickly moved away from the glacier and unloaded the frozen detrital materials in the process of transportation. The content of sand, silt and clay in the inner part of Kongsfjord showed obvious regularity, which can better indicate the source of the sediment brought by different ways such as icebergs, river input and so on (Shi et al., 2011). Based on the exponential decay law of $^{210}Pb_{ex}$, we estimated the sedimentary flux of the sediment core. In Fig. 3a, a significant piecewise-linearity phenomenon can be observed. It is unlikely that this relates to mixing because the mean grain size did not show an obvious mixing section (Fig. 2b). The highest sand content could indicate a dramatic incident that resulted in the deposition of coarse particles in fjord and coastal environments. The terrigenous input carried coarse particles into the fjord but decreased over time, as indicating by the reduction in the sand content with mass depth (Fig. 2b). Thereafter, the sand content increased with the reduced mass depth, probably due to the rising influx of glacial debris resulting from climate change.

The constant flux constant sedimentation (CFCS) model was used here to calculate the mass accumulation rate (MAR) of each segment of the sediment core (Sanchez-Cabeza and Ruiz-Fernández, 2012):

$$\ln C_i = \ln C_0 - \frac{\lambda}{r} m(i), \tag{1}$$

where C_i is the activity (Bq/kg) of $^{210}Pb_{ex}$ in Section i, C_0 is the activity (Bq/kg) of $^{210}Pb_{ex}$ in the surface, $m(i)$ is the mass depth (g/cm^2) of Layer i, r is the average mass accumulation rate (g/(cm^2·a)), and λ is the decay constant of the radionuclide. A regression line equation ($y = a + kx$) can be obtained from Fig. 3a.

$$r = -\frac{\lambda}{k}, \tag{2}$$

$$t(i) = \frac{m(i)}{r}, \tag{3}$$

$$C_0 = \mathrm{e}^a, \tag{4}$$

$$C_0 = C_i / \mathrm{e}^{-\lambda \frac{m(i)}{r}}, \tag{5}$$

$$f = r \times C_0, \tag{6}$$

where k is the gradient of the regression line, a is the intercept of the regression line, $t(i)$ is the time of Layer i since its formation (a), and f is the $^{210}Pb_{ex}$ flux to the sediment surface.

Using Eq. (2), MARs of 0.34 g/(cm^2·a) and 0.103 g/(cm^2·a) were estimated for the upper and lower parts of the core, respectively. The age of each layer was then determined using the MARs. Considering the cutting interval, the age of the turning point was (1995±2) years old. The errors of the $^{210}Pb_{ex}$ chronology were calculated using error propagation (Taylor and Thompson, 1998) considering the measurement errors of all the measured parameters in Eq. (2) and Eq. (3). Using Eq. (4), the C_0 for the upper part was 93 Bq/kg, while the C_0 for the lower part based on Eq. (5) was 121 Bq/kg. Meanwhile, we obtained the deposition fluxes of $^{210}Pb_{ex}$ during these two periods using Eq. (6), which were 316 Bq/(m^2·a) and 125 Bq/(m^2·a) for the upper and lower parts, respectively.

The results of the constant rate of supply model (CRS) were compared with those of the CFCS model. The fundamental hypothesis for the CRS model is that the f to the sediment surface are constant. The previous calculation suggested that the f value changed between these two stages (125 Bq/(m^2·a) and 316 Bq/(m^2·a)). Therefore, using the total integral of these two segments to calculate the MAR is more reliable. To depict the MAR

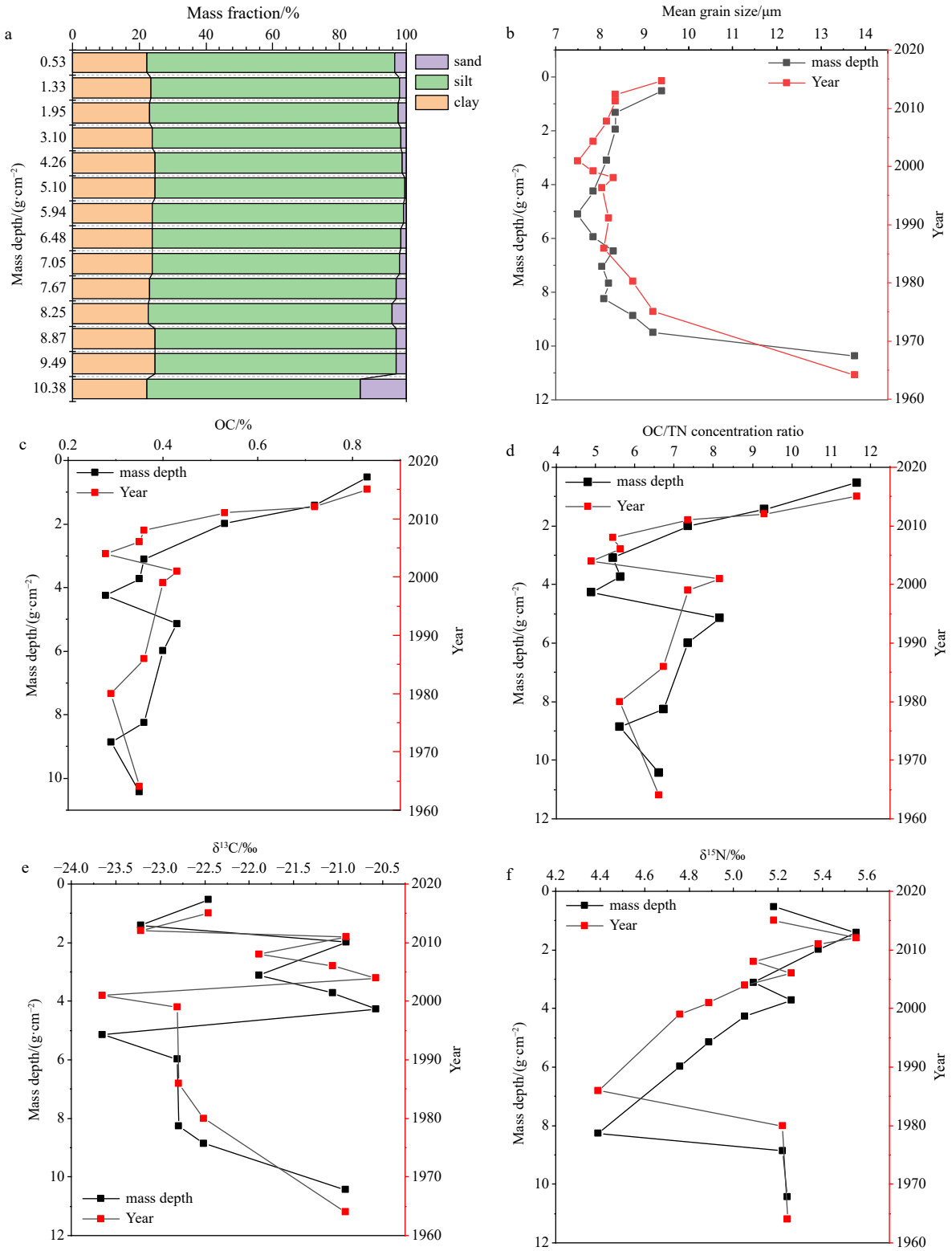

Fig. 2. Grain-size classification (a), mean grain size (b), organic carbon (OC) concentration (c), OC/total nitrogen (TN) concentration ratio (d), $\delta^{13}C$ (e) and $\delta^{15}N$ (f) in sediment Core Z3.

of each segment, the $^{210}Pb_{ex}$ activity in Core Z3 was pre-processed for the piecewise integration of the CRS (PICRS) model. It is feasible to lengthen the regression line to describe what happened before in the same state because the segments exhibited high linearity.

After extension, both segments were composed of fitted and measured parts. The MAR of the measured part was obtained by integrating the fitted and measured parts using the CRS model. The calculation formula of the CRS model is as follows (Sanchez-Cabeza and Ruiz-Fernández, 2012):

Table 1. Basic parameters for the Core Z3

Sample name	Mass depth/ (g·cm^{-2})	δ^{13}C/ ‰	δ^{15}N/ ‰	OC/ %	TN/ %	OC/ TN
Z3 0–1.0 cm	0.53	−22.46	5.18	0.83	0.07	11.65
Z3 1.0–1.5 cm	1.42	−23.22	5.55	0.72	0.08	9.30
Z3 1.5–2.0 cm	2.00	−20.91	5.38	0.53	0.07	7.36
Z3 2.5–3.0 cm	3.10	−21.89	5.09	0.36	0.07	5.45
Z3 3.0–3.5 cm	3.73	−21.06	5.26	0.35	0.06	5.63
Z3 3.5–4.0 cm	4.26	−20.58	5.05	0.28	0.06	4.89
Z3 4.0–5.0 cm	5.15	−23.65	4.89	0.43	0.05	8.16
Z3 5.0–5.5 cm	5.99	−22.81	4.76	0.40	0.05	7.35
Z3 7.0–7.5 cm	8.25	−22.79	4.39	0.36	0.05	6.73
Z3 7.5–8.0 cm	8.87	−22.51	5.22	0.29	0.05	5.62
Z3 8.5–9.5 cm	10.42	−20.92	5.24	0.35	0.05	6.61

Note: OC represents organic carbon concentration; TN, total nitrogen concentration; OC/TN, OC/TN concentration ratio.

$$A(i) = \int_{m_{i+1}}^{\infty} C_i \mathrm{d}m, \tag{7}$$

where $A(i)$ is the accumulative activity of $^{210}Pb_{ex}$ below Layer i (Bq/m^2), C_i is the $^{210}Pb_{ex}$ activity in Layer i (Bq/kg), and m_i is the mean mass depth of Section i (kg/m^2). Considering the actual sampling situation, the inventory of $^{210}Pb_{ex}$ can be written as follows:

$$A(0) = \sum_{i=1}^{n} C_i m_i, \tag{8}$$

$$t(i) = \frac{1}{\lambda} \ln \frac{A(0)}{A(i)}, \tag{9}$$

$$r(i) = \frac{\lambda A(i)}{C(i)}, \tag{10}$$

where $r(i)$ is the MAR of Layer i (kg/(m^2·a)), and n represents the last section.

The age of each layer was calculated using Eq. (9), and the turning point was (1995±2) years old. The determined ages were generally well matched between the CFCS and PICRS models, except that the lower part was slightly different (Fig. 3c). We also used the CRS model to integrate these two parts into a whole. However, the results were significantly different from the CFCS and PICRS models (Fig. 3c); therefore, we chose the CFCS and PICRS models to calculate the MAR.

Based on the $^{210}Pb_{ex}$ sedimentation rate, we found that there was an inconspicuous peak (Fig. 3d) observed in sediment Core Z3 correspond to 1986. It was not surprising because many studies have showed that the Chernobyl accident signal was recorded in the ice core and sediment core of the Arctic region (Pinglot et al., 1994, 2001; Jaworowski et al., 1997; Pinglot et al., 2003; Larsen et al., 2010). Such unsharp peak of ^{137}Cs was caused by the pre-depositional migration of ^{137}Cs in marine sediment, which would significantly broaden the peak without changing its location (Klaminder et al., 2012; Ferreira et al., 2013; Wang et al., 2017). Thus, we can still use this broaden peak to date sediment. The calculated MAR using 1986 peak of ^{137}Cs was 0.267 g/(cm^2·a), which is consistent with the MAR calculated using $^{210}Pb_{ex}$.

Several studies on the MAR based on $^{210}Pb_{ex}$ have been conducted in different areas of Kongsfjord (Table 2). Overall, the MARs reported for the central area of Kongsfjord were less than

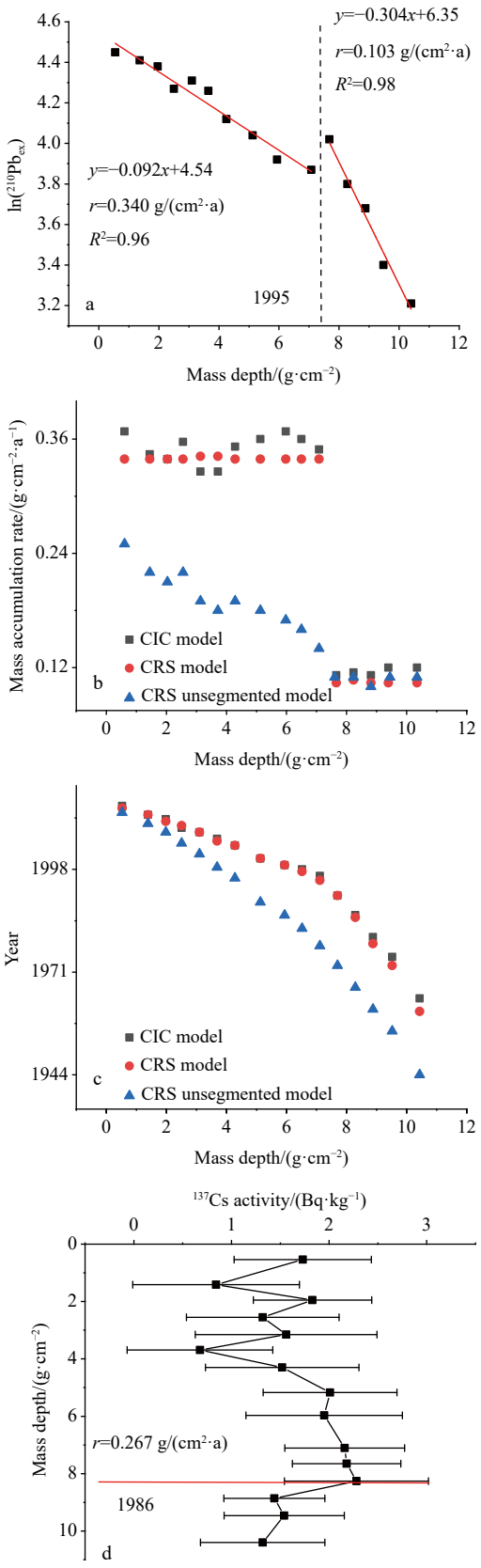

Fig. 3. Regression analysis model used for Core Z3 (a); comparison between the constant rate of supply (CRS), constant initial concentration (CIC), and CRS unsegmented models in terms of the mass accumulation rate (b) and dating results (c) for Core Z3; profile of ^{137}Cs in Core Z3 (d).

Table 2. Sedimentary rate of the sediment core from Kongsfjord

Study area	Sedimentation rate			Sampling time	Reference
	Inner part	Central part	Outer part		
Kongsfjord	–	0.103–0.340 g/(m²·a)	–	2017	this study
Kongsfjord	–	0.372–0.611 g/(m²·a)	–	–	Mohan et al. (2018)
Kongsfjord	>1.8 g/(m²·a)	0.18 g/(m²·a)	0.02 g/(m²·a)	2000	Aliani et al. (2004)
Kongsfjord	–	0.2 cm/a	0.13 cm/a	2015	Koziorowska et al. (2017)
Kongsfjord	–	2.5 cm/a (without regarding to mixing layer)	–	2000	Zaborska et al. (2006)
Kongsfjord	–	0.32 g/(m²·a)	0.13 g/(m²·a)	2009 and 2007	Kuliński et al. (2014)

Note: – represents no data.

1 g/(cm²·a), except for the MAR reported by Zaborska et al. (2006), who collected a core near the inner fjord. In addition, Mohan et al. (2018) reported that the MAR increased in last 20 a. This finding is similar to our results, whereby the sediment flux and $^{210}Pb_{ex}$ flux increased after (1995±2) a. This could be attributable to the increased influx of glacial meltwater containing debris since the mid-1990s.

4.2 *Inventories of $^{210}Pb_{ex}$ and ^{137}Cs*

The sources of $^{210}Pb_{ex}$ to Kongsfjord include atmospheric deposition, external seawater input, and glacial meltwater input. The sedimentary flux has increased over the past two decades; thus, some of the $^{210}Pb_{ex}$ sources have also changed. Previous studies from 1986 to 2006 (Dibb and Jaffrezo, 1993; Magand et al., 2006; Paatero et al., 2003; Samuelsson et al., 1986) reported that the atmospheric ^{210}Pb activity had no significant interannual variation from April to May in Ny-Ålesund, suggesting that atmospheric inputs of ^{210}Pb may not explain the variation in the $^{210}Pb_{ex}$ flux of seawater. The inventory of $^{210}Pb_{ex}$ in the sediment core was the integral of $^{210}Pb_{ex}$ versus the mass depth function [Eq. (7)]. The inventory of $^{210}Pb_{ex}$ in sediment Core Z3 (>6 517 Bq/m²) was much higher than that of atmospheric fallout (Table 3), further indicating that atmospheric fallout was not the main factor controlling the variation in the $^{210}Pb_{ex}$ flux. Hence, atmospheric fallout was not the main source of $^{210}Pb_{ex}$ in Kongsfjord.

In addition, $^{210}Pb_{ex}$ scavenging from open seawater is also relatively constant. The $^{210}Pb_{ex}$ inventory outside of the fjord was much higher than that in the middle of the fjord (Kuliński et al., 2014; Koziorowska et al., 2017) (Figs 4a, b). Our previous work showed that boundary scavenging contributed 55%–68% of sedimentary ^{210}Pb in Kongsfjord (Zeng et al., 2022). Thus, the high external value could relate to the boundary scavenging of ^{210}Pb from external seawater. The spatial distribution of coarse-grained components and the increasing grain size in the outer fjord indicate that sediment focusing occurred in the outer fjord (Zeng et al., 2022), which may correspond to the movement of sediment by gravity along the depth direction. The higher inventory of $^{210}Pb_{ex}$ in Core Z3 may also relate to sediment focusing. When the sediment particles are resuspended in seawater, ^{210}Pb is adsorbed by the sediment particles and finally buried in the bottom sediment. Previous studies undertaken in the Arctic Ocean have shown that boundary scavenging in the marginal sea region can provide a $^{210}Pb_{ex}$ flux that is several times higher or even an order of magnitude higher than that of ^{222}Rn decay in overlying water and atmospheric deposition (Kuzyk et al., 2013; Moore et al., 1973). In addition, as discussed above, the increase in terrigenous inputs from glacial meltwater would be another factor causing this higher inventory. Overall, the additional inputs from glacial meltwater, boundary scavenging, and sediment focusing enhanced the sedimentary inventory of ^{210}Pb relative to atmospheric fallout.

Unlike the distribution of $^{210}Pb_{ex}$, the inventory of ^{137}Cs in this study ((227±77) Bq/m²) was similar to the global fallout of ^{137}Cs at 70°–80°N (285 Bq/m²). The global fallout of ^{137}Cs at 70°–80°N was calculated by multiplying the fallout ^{90}Sr by a conversion factor of 1.6 (Aarkrog, 2003). The difference in these values relates to the fact that ^{137}Cs mainly exists in seawater and cannot be easily adsorbed by sediment particles that eventually settle out. Matishov et al. (2011) reported that the atmospheric flux of ^{137}Cs in the Barents Sea was 0.1 Bq/(m²·a) during 2000–2009. The corresponding inventory during this period was 4.7 Bq/m², which is clearly lower than our measured results. This suggests that the contribution of ^{137}Cs from atmospheric fallout during 2017–2018 was negligible. The ^{137}Cs activity in the seawater of the fjord was vertically uniform, indicating that ^{137}Cs is a relatively conservative nuclide in seawater (Gwynn et al., 2004). The sorption of ^{137}Cs from seawater to marine particles should be very small. Even in the presence of sediment focusing, the cycle of deposition/resuspension would not capture more ^{137}Cs from seawater. It has been reported that ^{137}Cs is tightly adsorbed onto the clay fraction, especially illite and kaolinite, in freshwater (Saiers and Hornberger, 1996; Hinton et al., 2006). Thus, terrestrial particulate matter was

Table 3. Inventories of $^{210}Pb_{ex}$ and ^{137}Cs (both values were decay-corrected to 2017)

Sample name	Location	Inventory/(Bq·m⁻²)		Reference
		$^{210}Pb_{ex}$	^{137}Cs	
Atmospheric fallout	70°–80°N	385–1 837	285	Aarkrog (2003); Zhang et al. (2021)
Svalbard	–	1 455–2 582	–	Appleby (2004)
Z3	78.95°N, 12.03°E	6 517±791	227±77	this study
KO	79.00°N, 11.48°E	17 766	–	Kuliński et al. (2014)
KM	78.94°N, 12.14°E	8 065	–	Kuliński et al. (2014)
kb1	79.02°N, 11.45°E	25 540	–	Koziorowska et al. (2017)
kb2	78.94°N, 11.98°E	18 571	–	Koziorowska et al. (2017)
V3	78.93°N, 12.37°E	>8 631	–	Svendsen et al. (2002)
KO-1	78.95°N, 12.03°E	10 464	–	Svendsen et al. (2002)

Note: – represents no data.

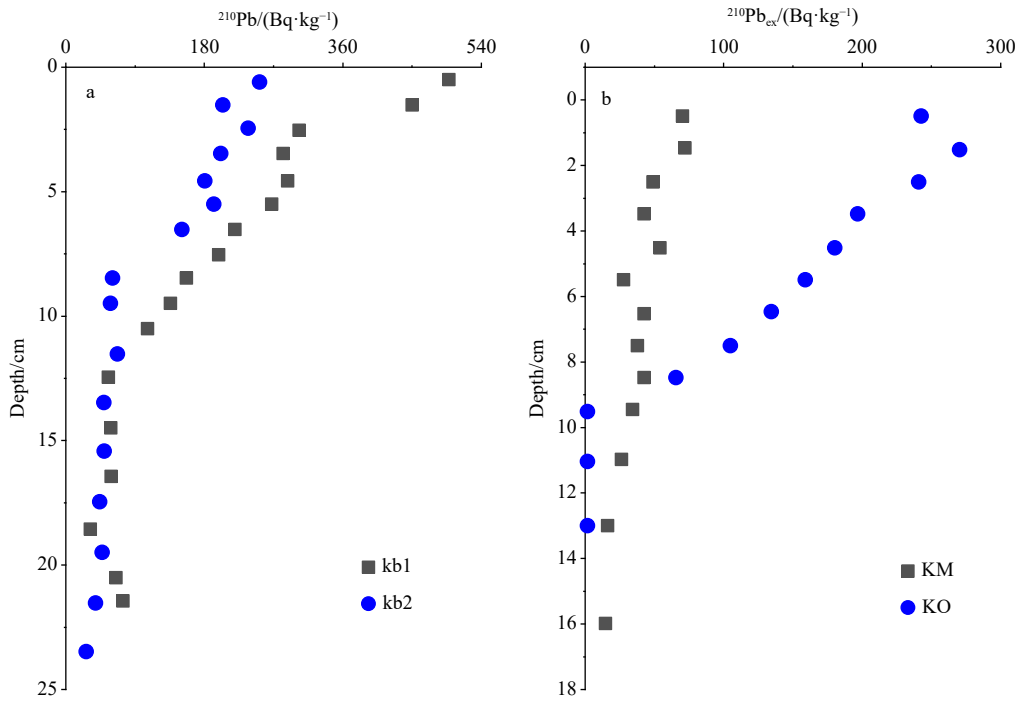

Fig. 4. Profiles of ^{210}Pb (a) and ^{210}Pb$_{ex}$ (b). Data in a and b are from Kuliński et al. (2014) and Koziorowska et al. (2017). The information of Stations KM, KO, kb1 and kb2 are presented in Table 3.

probably the main source of ^{137}Cs in fjord sediments. The similar sedimentary inventory of ^{137}Cs with atmospheric fallout could be attributable to terrigenous particles that adsorbed most fallout ^{137}Cs in freshwater systems.

4.3 *Distribution of OC, TN and source of organic matter*

The stable carbon, nitrogen and their isotopes could be used to identify the source of organic matter (OM) (Schubert and Calvert, 2001; Ogrinc et al., 2005). The distribution of carbon and nitrogen in the Kongsfjord sediment was reported in several previous studies. Terrestrially-derived OM had an OC/TN concentration ratio higher than 10 in the Arctic, due to the influence of C3 plants and ancient OM. The OM from marine sources displayed a lower OC/TN concentration ratio (i.e., <8) (Ruttenberg and Goñi, 1997; Naidu et al., 2000; Winkelmann and Knies, 2005). So, we can use the range of δ^{13}C and δ^{15}N to roughly assess the source of organic matter (Thornton and McManus, 1994; Andrews et al., 1998; Maksymowska et al., 2000; Carreira et al., 2002; Goñi et al., 2003; Gordon and Goñi, 2003; Meksumpun et al., 2005; Ogrinc et al., 2005; Voss et al., 2005; Usui et al., 2006; Barros et al., 2010). As shown in Fig. 5, both terrestrial and marine sources contributed to the organic matter in Core Z3.

The OC/TN concentration ratios of surface sediments in the inner part of Kongsfjord (typically 7–8) were indicative for a dominance of marine OM, and had no significant change in the spatial distribution pattern (Kim et al., 2011). Our results showed an increase trend from middle part to surface layer of Core Z3 (from 6 cm to 12 cm) which suggested more contribution of the terrestrial organic matter.

Briefly, for soils, mosses and debris of land vegetation, the $\delta^{13}C_{org}$ values ranged from –35 ‰ to –24.9 ‰; for glacier discharge water, the $\delta^{13}C_{org}$ values ranged from –24.4‰ to –25.4‰ (Kim et al., 2011; Kuliński et al., 2014). In fjord water, the $\delta^{13}C_{org}$ values of particulate organic matter (POM) ranged from –26.1‰ to –22. 8‰ (surface) and –25.2‰ to –23.8‰ (near bottom), with the average of –24.6‰ and –24.5 ‰, respectively (Zhu et al., 2016). Similar results in inner fjord water (from –25.9‰ to –21.4‰, average –23.5‰) were reported (D'Angelo et al., 2018). Significantly higher $\delta^{13}C_{org}$ was found in all sediment samples in this study than the reported terrestrial matter and close to the highest value of POM in fjord water (Zhu et al., 2016). The $\delta^{13}C_{org}$ values differed between the sediment in the vicinity of glacier front and other fjord sediment, which might correlate to the different sources of OM (Bourgeois et al., 2016).

The δ^{13}C variability in surface sediment is widely used to determine relative proportions of terrestrial and marine-derived organic matter by application of a two-end-member mixing model (Hedges et al., 1988; Schubert and Calvert, 2001; Winkelmann and Knies, 2005; Belicka and Harvey, 2009). Since terrestrial δ^{13}C and δ^{15}N end-members, especially δ^{13}C, are relatively constant in the Svalbard region (Winkelmann and Knies, 2005). According to previous studies in Svalbard region, we applied an average δ^{13}C value (–26.8‰) for terrigenous organic matter and marine organic matter (–20.6‰) in our equations (Winkelmann and Knies, 2005; Knies and Martinez, 2009; Koziorowska et al., 2016). Using these C isotope endmember values, we calculated the relative contribution of terrestrial OM (F_{terr}) to fjord sediments using the following equations:

$$\delta^{13}C_{sample} = F_{terr} \times \delta^{13}C_{terrestrial} + (1 - F_{terr}) \times \delta^{13}C_{marine}, \quad (11)$$

$$F_{terr} = \frac{\delta^{13}C_{sample} - \delta^{13}C_{marine}}{\delta^{13}C_{terrestrial} - \delta^{13}C_{marine}} \times 100\%, \quad (12)$$

where F_{terr} is the percentage of terrestrial organic carbon in the samples, $\delta^{13}C_{sample}$ is δ^{13}C measured in the samples, and $\delta^{13}C_{terrestrial}$ and $\delta^{13}C_{marine}$ are the end-member values for terrestrial and marine OM as provided above. The contributions of

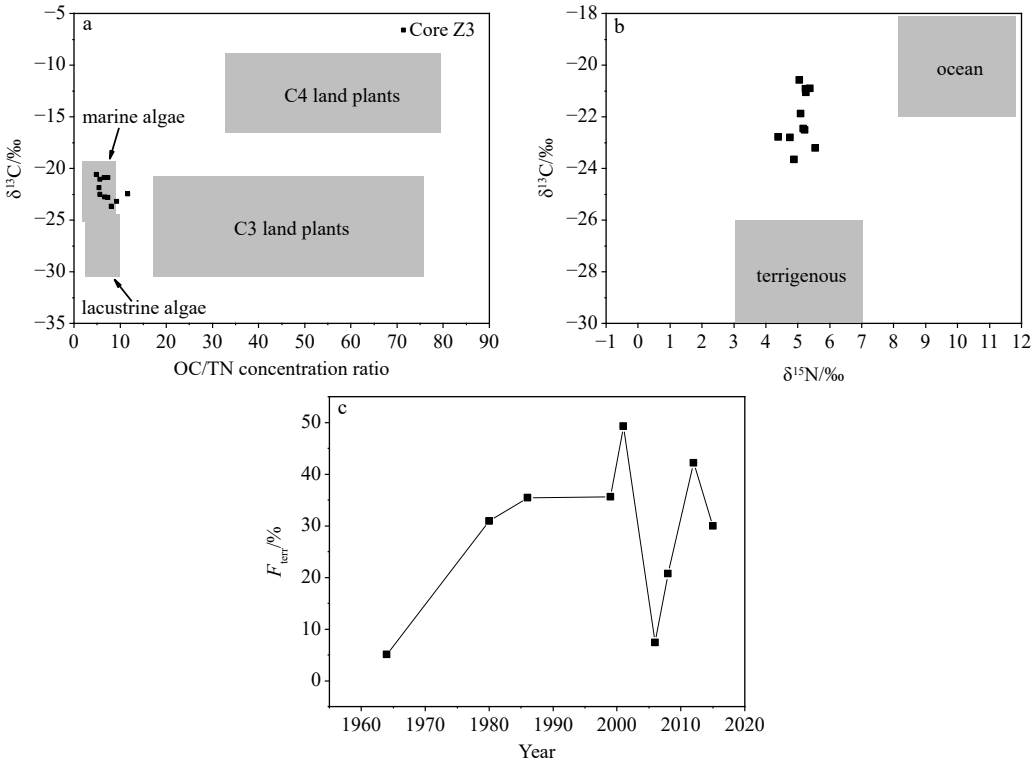

Fig. 5. Scatter plots for the $\delta^{13}C$, $\delta^{15}N$, organic carbon/total nitrogen (OC/TN) concentration ratio and the relative contribution of terrestrial organic matter (F_{terr}) in the Core Z3 (Meyers, 1994; Lamb et al., 2006; Barros et al., 2010).

marine and terrestrial organic matter were calculated using the two end-member approach [Eq. (11) and Eq. (12)]. The terrestrial organic matter contribution obtained for the Kongsfjord was in the range of 5%–49% (Fig. 5). The largest F_{terr} (49%) was observed in the middle part of Core Z3, which represented the year 2001. The estimated result of F_{terr} showed an overall increase trend from mid-1990s. The F_{terr} of 2000–2010 was small which might due to the enhancement of the Atlantic Current. Combining OC/TN concentration ratio and $\delta^{13}C$, we can conclude that the Kongsfjord area had been increasingly influenced by terrestrial matter since the mid-1990s.

In the inner part, the organic matter was derived mainly from benthic meiofauna and diatoms whereas in the mid and outer fjord it was derived mainly from prymnesiophyceae and zooplankton, like zooplankton fecal pellets (Bourgeois et al., 2016). The relatively higher $\delta^{13}C_{org}$ might be because the OM in sediment was strongly affected by marine OM. However based on the retene content and $\Delta^{14}C$ data in sediment, Kim et al. (2011) found that the ancient OM contribution in Konsfjorden sediments increased from 45%–50% in outside and middle fjord to 91% in inner fjord near the glacier front, and the values of Branched and Isoprenoid Tetraether suggested that the contribution of soil OM in Kongsfjord sediment is negligible. Minor component of soil OM in sediment is probably the reason of dyssynchrony between $\delta^{13}C_{org}$ and ^{137}Cs activity in sediment of Kongsfjord. Of course, as climate change, the biological activities on the land will become stronger, and the soil OM in the Kongsfjord will gradually increase, which will preferentially be observed in the region with higher activity of ^{137}Cs because it is less affected by the dilution of glacier matter. In Core Z3, the $\delta^{13}C_{org}$ didn't show a clear variation trend with the mass depth, but the concentration of organic carbon decreased on the top 2.84 g/cm^2 and then was substantially constant (Fig. 2c). This indicates that the increase in sediment flux didn't dilute the organic matter concentration of sediment, which means the deposited flux of organic matter in the water had increased due to the rise of MAR. Finally, the stable carbon, nitrogen and their isotopes suggested more terrestrial OM had been buried in Kongsfjord.

4.4 *Record of climate change in Kongsfjord*

Fjords are vital systems in the Arctic and serve as an important point to evaluate the cause and effect of environmental change. The rate of sediment production and sedimentation in fjords is influenced by glacier fronts, fjord walls, side streams, and other topographical factors (Zaborska et al., 2006; Zajaczkowski, 2008). Kongsfjord is a glacial fjord located in the European Arctic on the west Spitsbergen coast in the Svalbard archipelago. Due to the influence of the North Atlantic Current, Kongsfjord has a significantly warmer climate than other environments at the same latitude (Promińska et al., 2017). This might lead to increased calving of tidewater glaciers and occasionally accelerated glacier retreat and more meltwater in the Kongsfjord (Husum et al., 2019; Luckman et al., 2015). The environment of Kongsfjord has been changing gradually under the influence of ongoing climate change. In our study, Core Z3 suggests an obvious increase in MAR since (1995±2) a, which may result from climate change in Ny-Ålesund. To better illustrate this phenomenon, we collected and collated published data.

Despite being relatively stable, the air temperature in Ny-Ålesund exhibited an overall warming trend since the 1960s, and continued to increase after 1994 (Fig. 6b). With the increase in temperature, glacier melting began to accelerate in the mid-late 1990s. Such climate change might lead to a sedimentation rate increase during recent decades. In the South Shetland Islands, Boldt et al. (2013) reported that climate change resulted in a 2-to-4-fold increase in the MAR for three proximal ice cores. The res-

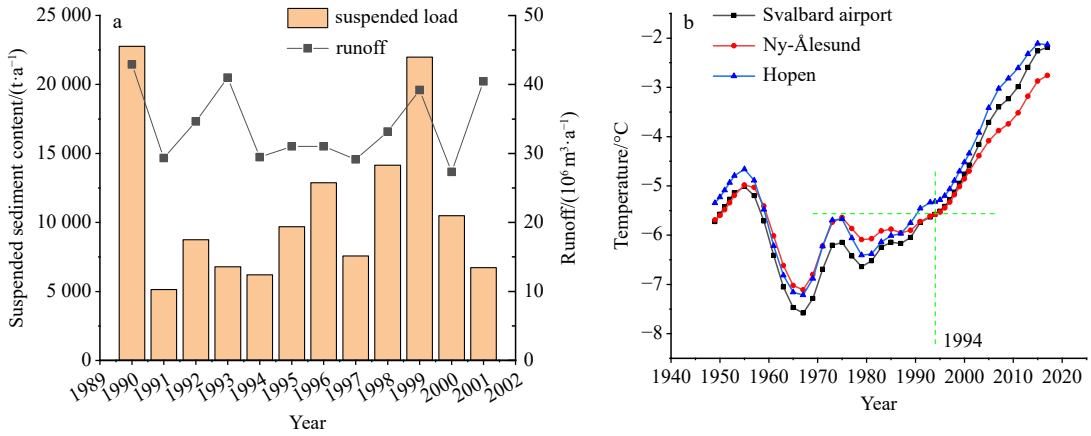

Fig. 6. Sediment transport in Bayelva River (a) and air temperature in Ny-Ålesund (b) over time. Data in a are from Bogen and Bønsnes (2003), data in b are from http://www.mosj.no/en/climate/.

ults of Mohan et al. (2018) showed that the sedimentation rate had increased to (0.34 cm/a) during the last 20 a, which may have related to the increased influx of glacial meltwater containing debris. Local climate warming accelerated the retreat of these glaciers, and the mineral materials eroded by them were transported to Kongsfjord (Koppes et al., 2015). During 1996–2000, the average annual content of suspended particulate matter (SPM) transported by the Bayelva River increased slightly compared with 1990–1995 (from 7 697 t/a to 10 374 t/a, Fig. 6a). This suggested that sediment availability increased because there was no significant increase in the annual average runoff (Bogen and Bønsnes, 2003). The increase in the transport of glacial debris into Kongsfjord may have resulted in the higher sediment fluxes that were observed in Core Z3. This rate can be well supported by the studies done on glacier surface speed and frontal ablation. Also, the frontal ablation has changed from 0.088 Gt/a (Lefauconnier et al., 1994) to 0.14–0.16 Gt/a (Schellenberger et al., 2015). The retreat and frontal ablation might have influenced the sediment deposition pattern in the inner part glacial front regions of Kongsfjord and it reflected in the core taken in the present study also. In short, climate change in Kongsfjord had intensified since the mid-to-late 1990s. Consequently, the acceleration in glacial melting had led to more sediment input into the adjacent fjord. The OC/TN concentration ratio and OC of Core Z3 also increased after 1997, indicating an increase in the terrigenous organic matter concentration corresponding to glacial ablation. The ^{137}Cs activity in Core Z3 also increased slightly after 1997. These observations suggested an increase input of terrigenous materials largely related to glacial ablation which increased the sedimentary particles released from melting glacier and eroded from continent by melting water.

In addition to the change in the sediment flux, the $^{210}Pb_{ex}$ flux estimated from Core Z3 increased from 125 Bq/(m^2·a) to 316 Bq/(m^2·a). As discussed earlier, the increase in the radionuclide flux in Core Z3 probably resulted from glacier inputs. Two reasons may explain this phenomenon: (1) the accelerated melting of glaciers caused more $^{210}Pb_{ex}$ to be released by glaciers, and (2) the contents of coarse and fine particles in the debris transported by glaciers increased. As the adsorption capability of fine particles is better than that of coarse particles (He and Walling, 1996), $^{210}Pb_{ex}$ will be more concentrated on fine particles, which are easily transported by meltwater. With the shift in the composition of SPM, more $^{210}Pb_{ex}$ would be introduced into Kongsfjord. Briefly, all collected data, including the samples of Core Z3, indicate that climate change in Ny-Ålesund has intensified since the mid-late 1990s, thus accelerating glacier melting and leading to increases in the OC/TN concentration ratio, sediment MAR, and $^{210}Pb_{ex}$ flux in Kongsfjord.

5 Conclusions

By observing the sedimentary records of radionuclides, organic carbon, and nitrogen in a sediment core collected from Kongsfjord in the Arctic during August 2017, we drew the following conclusions. After the mid-late 1990s, the MAR of Core Z3 increased from 0.103 g/(m^2·a) to 0.340 g/(m^2·a), while the $^{210}Pb_{ex}$ flux increased from 125 Bq/(m^2·a) to 316 Bq/(m^2·a), suggesting that two separate periods should be considered in the CRS model. A comparison between the atmospheric input of $^{210}Pb_{ex}$ and the inventory of $^{210}Pb_{ex}$ indicated that the main sources of $^{210}Pb_{ex}$ to the inside area of Kongsfjord were probably sediment focusing, boundary scavenging, and increased riverine input originating primarily from glacial meltwater. Considering that ^{137}Cs is relatively conservative in seawater and that the inventory of ^{137}Cs was similar to the global fallout of ^{137}Cs, terrestrial inputs were the main source of ^{137}Cs in fjord sediments. The maximum OC/TN concentration ratio in the top layer of Core Z3 indicates the influence of terrestrial OM. Combining δ^{13}C, δ^{15}N and OC/TN concentration ratio, we can conclude that the relative contribution of terrestrial organic matter showed an increased trend since mid-1990s. The trends in the variation in the MAR, the acceleration of glacier melting, the increase in SPM in the Bayelva River, and the rise in temperature were similar, suggesting that the change in the sedimentary environment in Kongsfjord is the result of climate change in Ny-Ålesund. All results of our study indicated that the temperature-driven glacial melting could release more OM originating from the meltwater or terrestrial materials and significantly reconstructed the sedimentary environment in Konsfjorden.

Acknowledgements

We thank two anonymous reviewers for their constructive comments for improvement of the original manuscript. We thank Zhuoyi Zhu for his assistance with field sampling.

References

Aarkrog A. 2003. Input of anthropogenic radionuclides into the World Ocean. Deep-Sea Research Part II: Topical Studies in Oceanography, 50(17–21): 2597–2606, doi: 10.1016/s0967-0645(03)

00137-1
Aliani S, Bartholini G, Degl'innocenti F, et al. 2004. Multidisciplinary investigations in the marine environment of the inner Kongsfiord, Svalbard Islands (September 2000 and 2001). Chemistry and Ecology, 20(S1): S19–S28, doi: 10.1080/02757540410001655396
Andreassen K, Hubbard A, Winsborrow M, et al. 2017. Massive blow-out craters formed by hydrate-controlled methane expulsion from the Arctic seafloor. Science, 356(6341): 948–953, doi: 10.1126/science.aal4500
Andrews J E, Greenaway A M, Dennis P F. 1998. Combined carbon isotope and C/N ratios as indicators of source and fate of organic matter in a poorly flushed, tropical estuary: Hunts Bay, Kingston Harbour, Jamaica. Estuarine, Coastal and Shelf Science, 46(5): 743–756, doi: 10.1006/ecss.1997.0305
Appleby P G. 2004. Environmental change and atmospheric contamination on Svalbard: sediment chronology. Journal of Paleolimnology, 31(4): 433–443, doi: 10.1023/B:JOPL.0000022545.73163.ed
Barros G V, Martinelli L A, Novais T M O, et al. 2010. Stable isotopes of bulk organic matter to trace carbon and nitrogen dynamics in an estuarine ecosystem in Babitonga Bay (Santa Catarina, Brazil). Science of the Total Environment, 408(10): 2226–2232, doi: 10.1016/j.scitotenv.2010.01.060
Belicka L L, Harvey H R. 2009. The sequestration of terrestrial organic carbon in Arctic Ocean sediments: A comparison of methods and implications for regional carbon budgets. Geochimica et Cosmochimica Acta, 73(20): 6231–6248, doi: 10.1016/j.gca.2009.07.020
Bendixen M, Iversen L L, Bjørk A A, et al. 2017. Delta progradation in Greenland driven by increasing glacial mass loss. Nature, 550(7674): 101–104, doi: 10.1038/nature23873
Berge J, Heggland K, Lønne O J, et al. 2015. First records of Atlantic mackerel (*Scomber scombrus*) from the Svalbard Archipelago, Norway, with possible explanations for the extension of its distribution. Arctic, 68(1): 54–61, doi: 10.14430/arctic4455
Bogen J, Bønsnes T E. 2003. Erosion and sediment transport in High Arctic rivers, Svalbard. Polar Research, 22(2): 175–189, doi: 10.3402/polar.v22i2.6454
Boldt K V, Nittrouer C A, Hallet B, et al. 2013. Modern rates of glacial sediment accumulation along a 15°S-N transect in fjords from the Antarctic Peninsula to southern Chile. Journal of Geophysical Research: Earth Surface, 118(4): 2072–2088, doi: 10.1002/jgrf.20145
Bourgeois S, Kerhervé P, Calleja M L, et al. 2016. Glacier inputs influence organic matter composition and prokaryotic distribution in a high Arctic fjord (Kongsfjorden, Svalbard). Journal of Marine Systems, 164: 112–127, doi: 10.1016/j.jmarsys.2016.08.009
Box J E, Colgan W T, Christensen T R, et al. 2019. Key indicators of Arctic climate change: 1971–2017. Environmental Research Letters, 14(4): 045010, doi: 10.1088/1748-9326/aafc1b
Carreira R S, Wagener A L R, Readman J W, et al. 2002. Changes in the sedimentary organic carbon pool of a fertilized tropical estuary, Guanabara Bay, Brazil: an elemental, isotopic and molecular marker approach. Marine Chemistry, 79(3–4): 207–227, doi: 10.1016/s0304-4203(02)00065-8
Choudhary S, Nayak G N, Khare N. 2020. Source, mobility, and bioavailability of metals in fjord sediments of Krossfjord-Kongsfjord system, Arctic, Svalbard. Environmental Science and Pollution Research, 27(13): 15130–15148, doi: 10.1007/s11356-020-07879-1
Christiansen H H, Etzelmüller B, Isaksen K, et al. 2010. The thermal state of permafrost in the Nordic area during the international polar year 2007–2009. Permafrost and Periglacial Processes, 21(2): 156–181, doi: 10.1002/ppp.687
Cowan E A, Seramur K C, Powell R D, et al. 2010. Fjords as temporary sediment traps: history of glacial erosion and deposition in Muir Inlet, Glacier Bay National Park, southeastern Alaska. Geological Society of America Bulletin, 122(7–8): 1067–1080, doi: 10.1130/b26595.1
D'Angelo A, Giglio F, Miserocchi S, et al. 2018. Multi-year particle fluxes in Kongsfjorden, Svalbard. Biogeosciences, 15(17): 5343–5363, doi: 10.5194/bg-15-5343-2018
Dibb J E, Jaffrezo J L. 1993. Beryllium-7 and lead-210 in aerosol and snow in the Dye 3 gas, aerosol and snow sampling program. Atmospheric Environment. Part A. General Topics, 27(17–18): 2751–2760, doi: 10.1016/0960-1686(93)90307-K
Du Jinzhou, Wu Ying, Huang Dekun, et al. 2010. Use of ^{7}Be, ^{210}Pb and ^{137}Cs tracers to the transport of surface sediments of the Changjiang Estuary, China. Journal of Marine Systems, 82(4): 286–294, doi: 10.1016/j.jmarsys.2010.06.003
Ferreira P A D L, Ribeiro A P, Nascimento M G D, et al. 2013. ^{137}Cs in marine sediments of Admiralty Bay, King George Island, Antarctica. Science of the Total Environment, 443: 505–510, doi: 10.1016/j.scitotenv.2012.11.032
Goldberg E D. 1963. Geochronology with ^{210}Pb. In: Radioactive Dating. Vienna: IAEA, 121–131
Goñi M A, Teixeira M J, Perkey D W. 2003. Sources and distribution of organic matter in a river-dominated estuary (Winyah Bay, SC, USA). Estuarine, Coastal and Shelf Science, 57(5–6): 1023–1048, doi: 10.1016/s0272-7714(03)00008-8
Gordon E S, Goñi M A. 2003. Sources and distribution of terrigenous organic matter delivered by the Atchafalaya River to sediments in the northern Gulf of Mexico. Geochimica et Cosmochimica Acta, 67(13): 2359–2375, doi: 10.1016/s0016-7037(02)01412-6
Gwynn J P, Dowdall M, Davids C, et al. 2004. The radiological environment of Svalbard. Polar Research, 23(2): 167–180, doi: 10.1111/j.1751-8369.2004.tb00006.x
He Qing, Walling D E. 1996. Interpreting particle size effects in the adsorption of ^{137}Cs and unsupported ^{210}Pb by mineral soils and sediments. Journal of Environmental Radioactivity, 30(2): 117–137, doi: 10.1016/0265-931x(96)89275-7
Hedges J I, Clark W A, Come G L. 1988. Organic matter sources to the water column and surficial sediments of a marine bay. Limnology and Oceanography, 33(5): 1116–1136, doi: 10.4319/lo.1988.33.5.1116
Hinton T G, Kaplan D I, Knox A S, et al. 2006. Use of illite clay for *in situ* remediation of ^{137}Cs-contaminated water bodies: field demonstration of reduced biological uptake. Environmental Science & Technology, 40(14): 4500–4505, doi: 10.1021/es060124x
Hodgkins R, Bryant R, Darlington E, et al. 2016. Pre-melt-season sediment plume variability at Jökulsárlón, Iceland, a preliminary evaluation using *in-situ* spectroradiometry and satellite imagery. Annals of Glaciology, 57(73): 39–46, doi: 10.1017/aog.2016.20
Husum K, Howe J A, Baltzer A, et al. 2019. The marine sedimentary environments of Kongsfjorden, Svalbard: an archive of polar environmental change. Polar Research, 38: 3380, doi: 10.33265/polar.v38.3380
Jaworowski Z, Hoff P, Hagen J O, et al. 1997. A highly radioactive Chernobyl deposit in a Scandinavian Glacier. Journal of Environmental Radioactivity, 35(1): 91–108, doi: 10.1016/S0265-931X(96)00004-5
Kim J H, Peterse F, Willmott V, et al. 2011. Large ancient organic matter contributions to Arctic marine sediments (Svalbard). Limnology and Oceanography, 56(4): 1463–1474, doi: 10.4319/lo.2011.56.4.1463
Klaminder J, Appleby P, Crook P, et al. 2012. Post-deposition diffusion of ^{137}Cs in lake sediment: implications for radiocaesium dating. Sedimentology, 59(7): 2259–2267, doi: 10.1111/j.1365-3091.2012.01343.x
Knies J, Martinez P. 2009. Organic matter sedimentation in the western Barents Sea region: terrestrial and marine contribution based on isotopic composition and organic nitrogen content. Norwegian Journal of Geology, 89: 79–89
Koide M, Soutar A, Goldberg E D. 1972. Marine geochronology with ^{210}Pb. Earth and Planetary Science Letters, 14(3): 442–446, doi: 10.1016/0012-821x(72)90146-x
Koppes M, Hallet B, Rignot E, et al. 2015. Observed latitudinal variations in erosion as a function of glacier dynamics. Nature, 526(7571): 100–103, doi: 10.1038/nature15385

Koziorowska K, Kuliński K, Pempkowiak J. 2016. Sedimentary organic matter in two Spitsbergen fjords: terrestrial and marine contributions based on carbon and nitrogen contents and stable isotopes composition. Continental Shelf Research, 113: 38–46, doi: 10.1016/j.csr.2015.11.010

Koziorowska K, Kuliński K, Pempkowiak J. 2017. Distribution and origin of inorganic and organic carbon in the sediments of Kongsfjorden, Northwest Spitsbergen, European Arctic. Continental Shelf Research, 150: 27–35, doi: 10.1016/j.csr.2017.08.023

Krishnaswamy S, Lal D, Martin J M, et al. 1971. Geochronology of lake sediments. Earth and Planetary Science Letters, 11(1–5): 407–414, doi: 10.1016/0012-821X(71)90202-0

Kuliński K, Kędra M, Legeżyńska J, et al. 2014. Particulate organic matter sinks and sources in high Arctic fjord. Journal of Marine Systems, 139: 27–37, doi: 10.1016/j.jmarsys.2014.04.018

Kuzyk Z Z A, Gobeil C, Macdonald R W. 2013. ^{210}Pb and ^{137}Cs in margin sediments of the Arctic Ocean: controls on boundary scavenging. Global Biogeochemical Cycles, 27(2): 422–439, doi: 10.1002/gbc.20041

Lamb A L, Wilson G P, Leng M J. 2006. A review of coastal palaeoclimate and relative sea-level reconstructions using δ^{13}C and C/N ratios in organic material. Earth-Science Reviews, 75(1–4): 29–57, doi: 10.1016/j.earscirev.2005.10.003

Larsen J, Appleby P G, Christensen G N, et al. 2010. Historical and geographical trends in sediment chronology from lakes and marine sites along the Norwegian coast. Water, Air, and Soil Pollution, 206(1–4): 237–250, doi: 10.1007/s11270-009-0099-4

Lefauconnier B, Hagen J O, Rudant J P. 1994. Flow speed and calving rate of Kongsbreen glacier, Svalbard, using SPOT images. Polar Research, 13(1): 59–65, doi: 10.1111/j.1751-8369.1994.tb00437.x

Luckman A, Benn D I, Cottier F, et al. 2015. Calving rates at tidewater glaciers vary strongly with ocean temperature. Nature Communications, 6(1): 8566, doi: 10.1038/ncomms9566

Lydersen C, Assmy P, Falk-Petersen S, et al. 2014. The importance of tidewater glaciers for marine mammals and seabirds in Svalbard, Norway. Journal of Marine Systems, 129: 452–471, doi: 10.1016/j.jmarsys.2013.09.006

Magand O, Ferrari C, Gauchard P A, et al. 2006. Analysis of ^{7}Be and ^{210}Pb air concentrations in Ny-Ålesund, Svalbard: CHIMERPOL II project, preliminary results. Memoirs of National Institute of Polar Research, 59: 96–115

Maksymowska D, Richard P, Piekarek-Jankowska H, et al. 2000. Chemical and isotopic composition of the organic matter sources in the Gulf of Gdansk (Southern Baltic Sea). Estuarine, Coastal and Shelf Science, 51(5): 585–598, doi: 10.1006/ecss.2000.0701

Matishov G G, Matishov D G, Usyagina I S, et al. 2011. Assessment of ^{137}Cs and ^{90}Sr fluxes in the Barents Sea. Doklady Earth Sciences, 439(2): 1190–1195, doi: 10.1134/s1028334x11080265

Meksumpun S, Meksumpun C, Hoshika A, et al. 2005. Stable carbon and nitrogen isotope ratios of sediment in the gulf of Thailand: Evidence for understanding of marine environment. Continental Shelf Research, 25(15): 1905–1915, doi: 10.1016/j.csr.2005.04.009

Meyers P A. 1994. Preservation of elemental and isotopic source identification of sedimentary organic matter. Chemical Geology, 114(3–4): 289–302.

Mohan M, Sreelakshmi U, Sagar M K V, et al. 2018. Rate of sediment accumulation and historic metal contamination in a tidewater glacier fjord, Svalbard. Marine Pollution Bulletin, 131: 453–459, doi: 10.1016/j.marpolbul.2018.04.057

Moore H E, Poet S E, Martell E A. 1973. ^{222}Rn, ^{210}Pb, ^{210}Bi, and ^{210}Po profiles and aerosol residence times versus altitude. Journal of Geophysical Research, 78(30): 7065–7075, doi: 10.1029/JC078i030p07065

Mottram R, Simonsen S B, Svendsen S H, et al. 2019. An integrated view of Greenland ice sheet mass changes based on models and satellite observations. Remote Sensing, 11(12): 1407, doi: 10.3390/rs11121407

Naidu A S, Cooper L W, Finney B P, et al. 2000. Organic carbon isotope ratios (δ^{13}C) of Arctic Amerasian continental shelf sediments. International Journal of Earth Sciences, 89(3): 522–532, doi: 10.1007/s005310000121

Nilsen F, Skogseth R, Vaardal-Lunde J, et al. 2016. A simple shelf circulation model: intrusion of Atlantic water on the West Spitsbergen Shelf. Journal of Physical Oceanography, 46(4): 1209–1230, doi: 10.1175/jpo-d-15-0058.1

Ogrinc N, Fontolan G, Faganeli J, et al. 2005. Carbon and nitrogen isotope compositions of organic matter in coastal marine sediments (the Gulf of Trieste, N Adriatic Sea): indicators of sources and preservation. Marine Chemistry, 95(3–4): 163–181, doi: 10.1016/j.marchem.2004.09.003

Paatero J, Hatakka J, Holmén K, et al. 2003. Lead-210 concentration in the air at Mt. Zeppelin, Ny-Ålesund, Svalbard. Physics and Chemistry of the Earth, Parts A/B/C, 28(28–32): 1175–1180, doi: 10.1016/j.pce.2003.08.050

Pinglot J F, Hagen J O, Melvold K, et al. 2001. A mean net accumulation pattern derived from radioactive layers and radar soundings on Austfonna, Nordaustlandet, Svalbard. Journal of Glaciology, 47(159): 555–566, doi: 10.3189/172756501781831800

Pinglot J F, Pourchet M, Lefauconnier B, et al. 1994. Natural and artificial radioactivity in the Svalbard Glaciers. Journal of Environmental Radioactivity, 25(1–2): 161–176, doi: 10.1016/0265-931x(94)90013-2

Pinglot J F, Vaikmäe R A, Kamiyama K, et al. 2003. Ice cores from Arctic sub-polar glaciers: chronology and post-depositional processes deduced from radioactivity measurements. Journal of Glaciology, 49(164): 149–158, doi: 10.3189/172756503781830944

Promińska A, Małgorzata C, Waldemar W. 2017. Kongsfjorden and Hornsund hydrography-comparative study based on a multiyear survey in fjords of west Spitsbergen. Oceanologia, 59(4): 397–412, doi: 10.1016/j.oceano.2017.07.003

Ruttenberg K C, Goñi M A. 1997. Phosphorus distribution, C: N: P ratios, and $\delta^{13}C_{oc}$ in Arctic, temperate, and tropical coastal sediments: tools for characterizing bulk sedimentary organic matter. Marine Geology, 139(1–4): 123–145, doi: 10.1016/S0025-3227(96)00107-7

Saiers J E, Hornberger G M. 1996. The role of colloidal kaolinite in the transport of cesium through laboratory sand columns. Water Resources Research, 32(1): 33–41, doi: 10.1029/95wr03096

Samuelsson C, Hallstadius L, Persson B, et al. 1986. ^{222}Rn and ^{210}Pb in the Arctic summer air. Journal of Environmental Radioactivity, 3(1): 35–54, doi: 10.1016/0265-931x(86)90048-2

Sanchez-Cabeza J A, Ruiz-Fernández A C. 2012. ^{210}Pb sediment radiochronology: an integrated formulation and classification of dating models. Geochimica et Cosmochimica Acta, 82: 183–200, doi: 10.1016/j.gca.2010.12.024

Schellenberger T, Dunse T, Kääb A, et al. 2015. Surface speed and frontal ablation of Kronebreen and Kongsbreen, NW Svalbard, from SAR offset tracking. The Cryosphere, 9(6): 2339–2355, doi: 10.5194/tcd-8-6193-2014

Schubert C J, Calvert S E. 2001. Nitrogen and carbon isotopic composition of marine and terrestrial organic matter in Arctic Ocean sediments: implications for nutrient utilization and organic matter composition. Deep-Sea Research Part I: Oceanographic Research Papers, 48(3): 789–810, doi: 10.1016/s0967-0637(00)00069-8

Shi Fengdeng, Cheng Zhenbo, Wu Yonghua, et al. 2011. The research on glacial-marine deposit types and sedimentary processes in the Arctic Kongsfjorden. Haiyang Xuebao (in Chinese), 33(2): 115–123

Svendsen H, Beszczynska-Møller A, Hagen J O, et al. 2002. The physical environment of Kongsfjorden-Krossfjorden, an Arctic fjord system in Svalbard. Polar Research, 21(1): 133–166, doi: 10.3402/polar.v21i1.6479

Taylor J R, Thompson W. 1998. An introduction to error analysis: the study of uncertainties in physical measurements. Physics Today, 51(1): 57–58, doi: 10.1063/1.882103

Thornton S F, McManus J. 1994. Application of organic carbon and nitrogen stable isotope and C/N ratios as source indicators of organic matter provenance in estuarine systems: evidence from

the Tay Estuary, Scotland. Estuarine, Coastal and Shelf Science, 38(3): 219–233, doi: 10.1006/ecss.1994.1015

Usui T, Nagao S, Yamamoto M, et al. 2006. Distribution and sources of organic matter in surficial sediments on the shelf and slope off Tokachi, western North Pacific, inferred from C and N stable isotopes and C/N ratios. Marine Chemistry, 98(2–4): 241–259, doi: 10.1016/j.marchem.2005.10.002

Voss M, Liskow I, Pastuszak M, et al. 2005. Riverine discharge into a coastal bay: A stable isotope study in the Gulf of Gdańsk, Baltic Sea. Journal of Marine Systems, 57(1–2): 127–145, doi: 10.1016/j.jmarsys.2005.04.002

Walkusz W, Kwasniewski S, Falk-Petersen S, et al. 2009. Seasonal and spatial changes in the zooplankton community of Kongsfjorden, Svalbard. Polar Research, 28(2): 254–281, doi: 10.1111/j.1751-8369.2009.00107.x

Wang Jinlong, Baskaran M, Niedermiller J. 2017. Mobility of ^{137}Cs in freshwater lakes: a mass balance and diffusion study of Lake St. Clair, Southeast Michigan, USA. Geochimica et Cosmochimica Acta, 218: 323–342, doi: 10.1016/j.gca.2017.09.017

Wickström S, Jonassen M O, Cassano J J, et al. 2020. Present temperature, precipitation, and rain-on-snow climate in Svalbard. Journal of Geophysical Research: Atmospheres, 125(14): e2019JD032155, doi: 10.1029/2019JD032155

Winkelmann D, Knies J. 2005. Recent distribution and accumulation of organic carbon on the continental margin west off Spitsbergen. Geochemistry, Geophysics, Geosystems, 6(9): Q09012, doi: 10.1029/2005gc000916

Zaborska A, Pempkowiak J, Papucci C. 2006. Some sediment characteristics and sedimentation rates in an Arctic Fjord (Kongsfjorden, Svalbard). Środkowo-Pomorskie Towarzystwo Naukowe Ochrony Środowiska, 8: 79–96

Zajaczkowski M. 2008. Sediment supply and fluxes in glacial and outwash fjords, Kongsfjorden and Adventfjorden, Svalbard. Polish Polar Research, 29(1): 59–72

Zeng Sheng, Deng Binbin, Wang Jinlong, et al. 2022. Distribution of gamma-ray radionuclides in surface sediments of the Kongsfjorden, Arctic: implications for sediment provenance. Acta Oceanologica Sinica, 41(1): 21–29, doi: 10.1007/s13131-021-1916-x

Zhang Fule, Wang Jinlong, Baskaran Mark, et al. 2021. A global dataset of atmospheric ^{7}Be and ^{210}Pb measurements: annual air concentration and depositional flux. Earth System Science Data, 13(6): 2963–2994, doi: 10.5194/essd-13-2963-2021

Zhu Zhuoyi, Wu Ying, Liu Sumei, et al. 2016. Organic carbon flux and particulate organic matter composition in Arctic valley glaciers: examples from the Bayelva River and adjacent Kongsfjorden. Biogeosciences, 13(4): 975–987, doi: 10.5194/bg-13-975-2016